Formulation and evaluation of transdermal nanogel for delivery of artemether

Petra O. Nnamani[1, 2] Agatha A. Ugwu[1], Ogechukwu H. Nnadi[1], Franklin C. Kenechukwu[1], Kenneth C. Ofokansi[1], Anthony A. Attama[1], and Claus-Michael Lehr[2, 3]

[1]Drug Delivery & Nanomedicine Research Group; Public Health & Environmental Sustainability Research Group, Department of Pharmaceutics, University of Nigeria, Nsukka, Enugu State, Nigeria
[2]Department of Drug Delivery, HIPS - Helmholtz Institute for Pharmaceutical Research Saarland, Saarbrücken, Germany;
[3]Department of Pharmacy, Saarland University, Saarbrücken, Germany

*Correspondence Email: petra.nnamani@unn.edu.ng; obiomaeze@yahoo.com;
Phone No. : +234 803 696 3979

Abstract

Artemether (ART) is second to artesunate in being the most widely used derivatives of artemisinin in combination therapy of malaria. Nanostructured lipid carrier (NLC) formulations were prepared following our previous report using optimized ART concentration of 0.25 g dissolved in 5 %w/v mixture of solid (Gelucire 43/01 and Phospholipon 85G) and liquid (Transcutol) lipids at 90 ◦C. An aqueous surfactant phase at 90 ◦C was added (dropwise) under magnetic stirring (1000 rpm) for 5 min. The pre-emulsion was speedily homogenized at 28,000 rpm for 15 min and further probe sonicated at 60 % amplitude (15 min). Resultant sample was cooled at room temperature and frozen at -80 °C prior to lyophilization. The freeze-dried sample was used for solid state characterization as well as in the formulation of transdermal nanogels using three polymers (Carbopol 971P, Poloxamer 407 and *Prosopis africana* peel powder) to embed the ART-NLC, using ethanol as a penetration enhancer. Transdermal ART-nanogels were characterized accordingly (physical examination, pH, drug content, rheology, spreadability, stability, particle size and morphology, skin irritation, *in vitro* and *ex vivo* skin permeation and analysis of permeation data), $P<0.05$. Results indicated that ART nanogels showed good encapsulation, drug release, pH-dependent swelling, stability and tolerability. Overall, ART-nanogels prepared from Poloxamer 407 showed the most desirable drug permeation, pH, swellability, spreadability, viscosity and transdermal antiplasmodial properties superior to PAPP-ANG>C971P-ANG. A two-patch/week concurrent application of the studied nanogels could offer 100% cure of malaria as a lower-dose (50 mg ART) patient-friendly regimen devoid of the drug's many side effects.

Graphical abstract

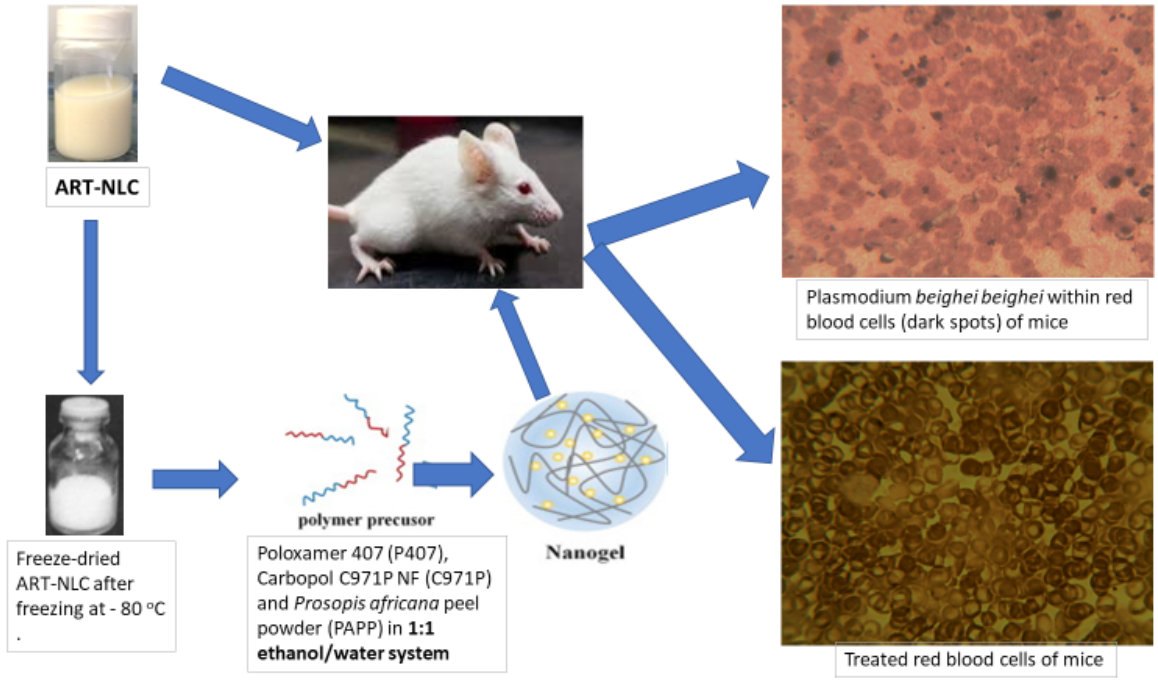

Keywords: Malaria; Artemether; Transdermal; Nanogel; Nanostructured lipid carrier; *Ex vivo* skin permeation

Introduction

In 2018, an estimated 228 million cases of malaria occurred worldwide (95% confidence interval [CI]: 206–258 million), compared with 251 million cases in 2010 (95% CI: 231–278 million) and 231 million cases in 2017 (95% CI: 211–259 million) [1]. Most malaria cases in 2018 were in the World Health Organization (WHO) African Region (213 million or 93%), followed by the WHO South-East Asia Region with 3.4% of the cases and the WHO Eastern Mediterranean Region with 2.1%. Nineteen countries in sub-Saharan Africa and India carried almost 85% of the global malaria burden [1]. Nigeria (25%) was among the six countries that accounted for more than half of all malaria cases worldwide followed by the Democratic Republic of the Congo (12%), Uganda (5%), and Cote d'Ivoire, Mozambique and Niger (4% each). Also reported is the fact that *Plasmodium falciparum* remains the most prevalent malaria parasite in the WHO African Region, accounting for 99.7% of estimated malaria cases in 2018, as

well as in the WHO South-East Asia Region (50%), the WHO Eastern Mediterranean Region (71%) and the WHO Western Pacific Region (65%) [1]. An estimated 405 000 deaths from malaria occurred globally, compared with 416 000 estimated deaths in 2017, and 585 000 in 2010. The most vulnerable group affected by malaria remains children under 5 years; who in 2018 accounted for 67% (272 000) of all malaria deaths worldwide [1]. Nearly 85% of global malaria deaths in 2018 were concentrated in 20 countries in the WHO African Region and India; Nigeria accounted for almost 24% of all global malaria deaths, followed by the Democratic Republic of the Congo (11%), the United Republic of Tanzania (5%), and Angola, Mozambique and Niger (4% each) [1]. The question is what is Nigeria not doing right despite the adoption of artemisinin-based combination therapy (ACT) in malaria treatment.

Artemisinin (ATM) and its derivatives have been used effectively in combination therapy for malaria treatment [1]. Despite antimalarial activities of these agents, they also have wide range of other biological activities including anti-inflammatory and anticancer effects [2, 3], antischistosomal activities [4], antimicrobial [5] and antiviral activities [6-8]. However, for malaria treatment, these rapidly-acting derivatives of artemisinin are usually combined with long-acting antimalarials (such as mefloquine, amodiaquine, sulfadoxine/pyrimethamine, lumefantrine, piperaquine, pyronaridine, chlorproguanil/dapsone) as artemisinin-based combination therapy (ACT), according to the WHO guideline [9-11]. ATMs generally inhibit gametocyte formation, increase cure rates and delay further transmission of resistant parasites [1, 12]. But their physicochemical properties affect their presentations and clinical performance, especially for the oil soluble artemether and the water-soluble artesunate and dihydroartemisinin (artenimol) [12]. To solve the issues regarding poor solubility and limited bioavailability of ATMs, nanoformulation has thus emerged as a promising strategy [13, 14]. A common consideration on nano ATMs design lies on their delivery and controlled release, where they are commonly regarded as hydrophobic drugs. Among these developments, is the design of a nanoformulation that can generate nanoparticles of these drugs for better performance than the conventional regimens (tablets, IM/IV injections, capsules, suppositories etc). A general method for their delivery is loading the drug molecules within a certain nanocarrier, which could be made from a wide array of materials (lipids and/or phospholipids [15-17], polymers [18, 19], mixed micelles [20], etc) and developed in the form of nanodispersions for various uses including skin application [12], oral application [13-21], buccal films [17] liquisolid compacts [16]. Additional chemistry for achieving site targeting and controllable drug release is often considered during the design [12, 22, 23]. Numerous nanosystems have been reported for ATMs delivery and controlled release, and those studies have been well-summarized in literature [13, 24].

Artemether (ART) for instance, is second to artesunate in being the most widely used derivatives of artemisinin for malaria treatment. Even though used as ACT, a lot of people have negative attitudes to taking ACT due to obvious side effects (nausea, vomiting, elevated SGPT and SGOT due to large doses) contributed by ART [12, 16]. Perhaps, this could be contributing to the current trends of resistance development to these important class of agents by *P. falciparum*. ART is a whitish yellow powder, potent rapidly-acting schizonticide, practically insoluble in water, belongs to BCS class II and has oral bioavailability of ~45%. Additionally, it has short half-life (1.5-3/5 h), melting point (86-88°C) and Log P (3.53). Nanotechnology offers the possibilities to overcome these drawbacks (poor solubility, low bioavailability, and extremely short half-life *in vivo*) [25, 26]. Our earlier work had demonstrated the possibility of administering ART as a sustained release topical agent using optimized nanostructured lipid carrier (NLC) regimen with adequate skin permeation over three days [12]. However, storage of such formulation may pose a problem in tropical countries with malaria endemicity. In terms of shelf stability, storage and distribution, ART-NLC may not be ideal and development of a more stable solid and/or semi-solid (e. g. nanogels) dosage platform is required for high patient compliance and easy storage, in addition to handling. To formulate NLC into dry form, freeze drying has been widely used as a standard method [27, 28]. Freeze drying prevents hydrolysis and physical degradation of phospholipids making up the matrix during extended storage. It has been shown that the use of cryoprotectants such as sugars (e.g. trehalose or sucrose), which form amorphous matrices (non-eutectic nature) help to protect the system from fusion and/or aggregation during freeze drying [27, 28]. Additionally, other bulking agents and/or stabilizers (e.g. lactose, mannitol, trehalose, hydroxyethyl starch and glycine) also aid in lyophilization by protecting the product especially when the product concentration is low and/or modify isotonicity (sucrose, trehalose, sorbitol and glycerol). We had previously reported on conversion of NLC into a more convenient oral delivery system as liquisolid compact to deliver poorly soluble drugs (artemether/lumefantrine) [16]. Therefore, the aim of this work was to exploit such excipients to formulate a semi-solid regimen (nanogels) for transdermal application of ART to the intact skin using nanoparticles generated from optimized NLC. These nanogels are expected to maintain the integrity, potency and function of the NLC as they would in the liquid dosage form. In other words, our objective was to produce a lower-dose (25 and/or 50 mg), more patient-friendly and stable transdermal semi-solid NLC-based nanogels for malaria treatment devoid of ART's side effects; as a once-a-week novel skin patch to prolong the release of the ordinarily fast-acting schizonticide ART (with short half-life, 1.5-3/5 h). This suggests therefore, that ART-nanogel patch could be used alone (in multiple

application sites as two skin patches/week, 50 mg) to cure malaria since this sustained release nanogel regimen would take care of recrudescence and development of resistance usually observed with the conventional single forms of ART and/or artemisinin, which the use of ACT as recommended by the WHO was meant to take care off.

2. Materials and methods

2.1. Materials

Artemether (ART) was procured from Ipca Laboratories Ltd., India. Gelucire® 43/01 Pellets and Transcutol® P were obtained from Gattefossé, France whereas Phospholipon® 85G (P85G) was donated by Lipoid GmbH, Germany. Tween® 80, sodium azide and sorbitol were obtained from Sigma-Aldrich, USA. Poloxamer 407 (Lutrol® F-127; BASF, Ludwigshafen, Germany) and Carbopol® 971P NF (The Lubrizol Corporation, USA) were equally gift samples. Propylene glycol, ethanol (Merck, Germany) and triethanolamine (Spectrum Chem. Mfg. Corp., California) were procured from local suppliers. All reagents were of analytical grade and used without further processing. Bi-distilled water was used throughout the study.

2.2. Preparation of NLC and nanogels

Hot homogenization/ultrasonication methods were used for NLC preparation according to an earlier report, but with modification [12]. Briefly, optimized ART (0.25 g) was added to lipid mixtures (5 %w/v) of Gelucire 43/01 (10 %), P85G (15%) and liquid lipid, Transcutol (75%) at 90 ◦C, and ethanol (44.6%) was subsequently added to the mixture. Surfactant (Tween 80®, 2 %) aqueous phase (44.6 %) at same temperature was added under magnetic stirring (1000 rpm) for 5 min. Pre-emulsion was generated using a homogeniser (Polytron PT 2500 E, Kinematica, USA) at 28,000 rpm for 15 min, probe sonicated (60 % amplitude, 15 min), cooled to room temperature and after 48 h, frozen at -80 °C prior to lyophilization (Martin Christ, Alpha 2-4 LSC GmbH, Osterode, Germany). Freeze-dried sample was used for solid state characterization.

Three polymers were recruited as bases for the freeze-dried NLC formulation containing ART to render it rheologically acceptable for dermal application, according to Table 1. Carbopol 971P NF (C971P), *Prosopis africana* peel powder (PAPP) and Poloxamer 407 (P407) were dissolved completely in pre-cooled purified water (5 °C). Ethanol (penetration enhancer) and propylene glycol (emollient) were added and mixed homogenously to

obtain smooth hydrogels. Freeze-dried NLC formulation (45 g, with or without drug) was added and thoroughly mixed to obtain nanogels. Triethanolamine was added (drops) to nanogels obtained from C971P to adjust pH to about 5.5. Plain hydrogels of each polymer were also prepared (without NLC). All formulations were kept at room temperature for 24 h to ensure no air-bubble formation, before dispensing in lacquered aluminum tubes (40 g), securely closed, and stored at room temperature until used. Nanogels were characterized accordingly.

Characterization of NLC particles

After NLC preparation, the particles were characterized with respect to their average size, size distribution, zeta potential (via electrophoretic mobility measurements) and polydispersity index. The particle size was measured with a Zetasizer Nano-ZS (Malvern Instruments, Worceshtire, UK). The zeta potential was calculated applying the Helmholtz–Smoluchowski equation (n = 3).

The particle morphology was studied with transmission electron microscope (TEM) and images were taken using a Zeiss EM 902 80 kV TEM with Henry-Casting Energy Filter and a GATAN Coolsnap500 CCD. For TEM images, NLC freeze-dried sample (10 mg) was diluted in 100 ml of distilled water, and 3µl sample was dropped on a carbon covered copper grid and dried overnight at room temperature.

Nanoparticle tracking analysis (NTA) is based on a laser illuminating microscopic technique and does not measure scattered light intensity compared to dynamic light scattering (DLS). In NTA, particles suspended in a fluid are excited by a laser, which scatters light, and hence, the particle position is determined under a microscope [12, 29]. These illuminated particles therefore exhibit Brownian motion and are analyzed by a camera in real-time and rate of the movement which is related solely to the viscosity of the liquid (0.89 cP), temperature (25.60 ºC), and size of the particles. Subsequently, each particle is simultaneously, but separately visualized and tracked from frame to frame by particle tracking image analysis software and the rate of particle movement is related to a sphere equivalent hydrodynamic diameter and calculated through a variation of Stokes-Einstein equation. For nanoparticle tracking analysis experiment, NLC samples were diluted 1:7000 with bi-distilled water. NTA was performed with digital microscope LM10HS system (NanoSight, Wiltshire, UK) and diluted samples were injected with sterile syringes (BD Discardit II, NJ, USA) into the sample chamber equipped with a 640 nm diode laser (red), then measured in a single shutter and gain mode for 90 s with manual shutter, gain, brightness, and threshold adjustments at room temperature. Particle video images moving under Brownian motion, were captured and analyzed by the NTA 2.0 image analysis software NanoSight LM10HS (NanoSight Ltd., Minton Park, Amesbury, Wiltshire SP47RT, UK),

635 nm laser with a high sensitivity camera (EMCCD). Triplicate measurements were done for each sample. The mean size and SD values obtained by the NTA software were based on the arithmetic values calculated with the sizes of all particles analyzed by the software to determine the D10, D50, D70, and D90 as number median diameters size distributions.

The degree of crystallinity and polymorphism of NLC particles were determined by differential scanning calorimetry (DSC Q100 TA Instrument, Germany) using sufficient quantities (5 mg) of drug and excipients, weighed in aluminum pan and heated from 25 to 150 °C at 10 °C/min under constant flushing with nitrogen (10 ml/min). DSC parameters of temperature onset, maximum peak, and enthalpy, were generated.

Encapsulation efficiency (EE) of ART-loaded NLC was determined by ultrafiltration according to an earlier established method [12]. Briefly, Vivaspin® filter tubes (Vivaspin, Germany) consisting sample donor chamber with basal filter membrane of molecular weight cut-off of 10,000 was used to hold a 2 ml aliquot of undiluted ART-NLC (upper chamber) while the sample recovery chamber was fixed at the lower compartment. The unit was tightly secured and centrifuged at 11,000 rpm for 2 h at 30 min intervals using a centrifuge (Model 420 R Rotina Hettich, Germany). The resultant filtrate was appropriately diluted with acetonitrile:water (90:10) and the amount of ART in the aqueous phase was estimated by a validated RP-HPLC. The EE and DL were calculated from the following equations:

$$\text{Encapsulation efficiency (\%)} = \frac{Real\ ART-loading}{Theoretical\ ART-loading} x\,100 \ldots\ldots\ldots\ldots\ldots\ldots\ldots\ldots\ldots\ldots Eq.(1)$$

$$\text{Drug loading (\%)} = \frac{Amount\ of\ encapsulated\ ART}{Total\ amount\ of\ ART \in formulation} x\,100 \ldots\ldots\ldots\ldots\ldots\ldots\ldots\ldots\ldots\ldots Eq.(2)$$

Briefly, HPLC determination of ART was done using a Dionex P680 HPLC pump (ASI-100 automated sample injector) equipped with UV/VIS detectors operating at 208 nm (210 and 214 nm). Samples were chromatographed on a stainless steel C18 reverse phase column (250 x 4.0 mm) packed with 5 µm particles (Lichrospher® 100 RP-18). Elution was done with the mobile phase of acetonitrile:water (90:10) at a flow rate of 40 µl /min at 40 °C for 5 min. A calibration curve was plotted for ART in the concentration range of 5-10 µg/ml. Percentage correlation

coefficient of 99.7904 % was reproducibly obtained from ART concentration and peak area of ART to estimate precision and accuracy of the HPLC method.

Ex vivo tape stripping study of ART-NLC formulation (0.250 g ART in NLC) was conducted by tape stripping of albino pig ear skin obtained from freshly slaughtered albino pigs from abattoir. Briefly, pig ear was mounted on an aluminum foil wrapped Teflon block, cleaned and secured with nails. Some 4 application sites were traced; 1 for zero-drug NLC (control) and 3 for test ART formulation at 15 µl application dose (containing 0.33 mg of ART) taken from a dispersion of NLC freeze-dried powder (2 g) formulation in 2 ml solvent mixture of acetonitrile/water (ACN/water 90/10). After application on the marked areas of the skin, the skin was incubated for 1 h in the oven under controlled conditions. Afterwards, *stratum corneum* layers were consecutively removed by tape stripping using an adhesive tape according to standard procedures [30-32]. The different tapes were extracted for 3 h in a shaker using the solvent mixture and quantified using a validated HPLC analytical method for ART content. All results were statistically analyzed.

Characterization of nanogels

Measurement of pH

The nanogels were examined for physical homogeneity, colour and consistency. Before use, each nanogel pH was always ascertained to ensure stability and skin convenience (pH 5.5). Briefly, a digital pH meter (Labtech, India) previously calibrated using standard buffer solutions (pH 4 and 7), was used to determine pH of nanogels in triplicate, and the average pH and standard deviation of each batch calculated. Direct immersion of pH meter electrode into samples immediately after formulation, 24 h post-pH adjustment then at 1, 3 and 6 months of storage were done.

Determination of spreadability

The nanogel formulation (1.0 g) was placed within a circle of 1.0 cm diameter on lower side of a pre-marked glass slide and another glass slide (unmarked) was placed over it, as modified from a previous report [33]. A weight of 200 g was placed on the upper glass slide for 5 min, then the diameter occupied by the spreading formulation was noted and spreadability was calculated in triplicate as follows:

$$\text{Spreadability (\%)} = \frac{Increase \in diameter}{Initial\, diameter} x\, 100 \ldots\ldots\ldots\ldots\ldots\ldots\ldots\ldots\ldots\ldots\ldots\ldots\ldots\ldots.. Eq.(3)$$

***In vitro* occlusivity**

A glass beaker (250 ml) containing distilled water (100 ml) covered with a filter paper (Whatmann No. 1) and secured in place with a rubber band was used. The nanogel (0.2 g) was distributed evenly on the filter paper and weight of the set-up ascertained. As a control, another glass beaker (250 ml) containing distilled water (100 ml) covered with filter paper was similarly weighed without applying any nanogel on it. Both glass beakers (test and control) were stored at 37 ± 0.5 °C for 48 h, after which their weight difference due to water evaporation through the filter paper were ascertained and applied to calculate occlusivity factor ‘F’ at 24 and 48 h as follows:

$$\text{Occlusivity factor, F} = 100[\frac{A-B}{A} ¿ \ldots\ldots\ldots\ldots\ldots\ldots\ldots\ldots\ldots\ldots\ldots\ldots... Eq.(4)$$

Where A (%) and B (%) are the water fluxes (% water loss) through the non-bearing and nanogel-bearing filters, respectively.

$$\text{Water loss (\%)} = \frac{Total\ water\ loss(g)}{Net\ weight\ of\ water} x\, 100 \ldots\ldots\ldots\ldots\ldots\ldots\ldots\ldots\ldots\ldots\ldots. Eq.(5)$$

Rheological evaluation

Viscosity determination of nanogels were done using a Brookfield viscometer (GallenKamp, England). Some quantities of nanogel (1, 3, and 5 g) were separately dispersed in 25 ml of 1:1 mixture of ethanol-purified water (1:1) and allowed an overnight hydration at room temperature before viscosity measurement. Triplicate determinations were carried out for validity of statistical analysis.

Drug content evaluation

The nanogel (1 g) was weighed and placed in a volumetric flask (100 ml) to which a mixture of ethanol-water (1:1) solution was added, mixed and sonicated for 30 min then made up to volume. This set up was centrifuged (4,000 rpm for 15 min), filtered using a membrane filter (0.45 µm, Mumbai, India) and drug content of the filtrate was determined spectrophotometrically (Jasco V-630 UV/VIS Double Beam, Japan), as modified from previous report

[16]. Briefly, 2 ml filtrate sample was added to 2 ml of concentrated HCl in a test tube, securely stoppered and stood in a water bath at 80 °C for 30 min and afterwards cooled, diluted with distilled water (25 ml) and filtered. Absorbance of this solution was taken at 345 nm against a blank solution of HCl (conc, 2 ml) made up to 25 ml with distilled water, according to the formula:

$$\text{Drug content} = \frac{Actual\ drug\ content}{Theoretical\ drug\ content} x\,100 \ldots\ldots\ldots\ldots\ldots\ldots\ldots\ldots\ldots\ldots Eq.(6)$$

***In vitro* drug release study from nanogels**

Direct contact of release medium with nanogel surface allows real-time determination of use-conditions. The membrane-free method was adopted and nanogel (1 g) was added to a graduated test tube placed in a water bath (Huanghua Instruments Co. Ltd., China) thermostatically maintained for 10 min. Pre-equilibrated release medium (1:1 ethanol-water mixture, 2.0 ml) was pre-equilibrated (37 ± 0.5 °C) and layered over the nanogel surface. The release medium was removed at pre-determined 5-hourly interval for 50 h and the test tube was cleared, weighed and layered with fresh medium to maintain sink condition, each time. This procedure was repeated for ART-NLC formulation as a positive control since there was no commercial sample of ART for skin use. All withdrawn samples were analyzed using earlier described spectrophotometric method. The amount of ART in nanogel samples was determined in triplicate according to the formula:

$$\text{Cumulative ART release rate} = \frac{Cumulative\ amount\ of\ ART\ released}{Initial\ amount\ of\ ART} \text{ x 100 \% } \ldots\ldots\ldots\ldots \text{ Eq. (7)}$$

Data obtained from *in vitro* release study were used for kinetic modeling. Model fitting into Higuchi, zero order, first order and Korsmeyer-Peppas was done to study the mechanism behind the release pattern of nanogels.

Animal care and use protocols

Randomly selected white albino Wistar rats weighing 210 – 250 g were procured from the animal house of Department of Pharmacology and Toxicology, Faculty of Pharmaceutical Sciences, University of Nigeria, Nsukka. Animals were humanely treated according to National Institute of Health (NIH Publications no. 8023, as revised in 1978) guidelines for animal care. They were housed in cages, fed standard rodent pellet (Guinea feeds Ltd, Nigeria), allowed free access to clean, fresh water in glass water bottles *ad libitum* and acclimatized for 1 week prior to study under a 12 h day/night cycle. Cage-side clinical observations was done throughout study period. All animal use

protocols were approved by the Animal Care and Use Committee of the Faculty of Pharmaceutical Sciences (approval no. FPSRE/UNN/18/00036), in compliance with the EU Directive 2010/63/EU for animal experiments.

Skin tolerance test

The skin tolerability of ART nanogel was carried out according to a previously described method [33, 34] with slight modifications. Generally, eleven rats weighing 200 – 220 g were used. Briefly, ART formulation groups (ART-NLC, C971P-ANG, PAPP-ANG and P407-ANG); placebo nanogels (C971P, PAPP and P407); plain hydrogels (C971P, PAPP and P407) and formaldehyde (1 %) solution (as positive control) were used. Some 24 h prior to experiment, rat dorsal skin was shaved with an electric clipper. All formulation was tested at 1 g dose (1 g of ART-nanogels contained 12.5 mg of ART whereas 1 g of ART-NLC contained 22 mg of ART) and was separately applied to the shaved dorsal side of the rats, uniformly spread (within an area of 0.4 cm^2) until complete absorption. The dorsal skin of the rat in positive control was treated with 1 % formaldehyde solution whereas all placebo nanogels (no ART) and plain hydrogels served as negative controls. These treatments were done once daily for 5 days and rat skin was observed for any visible change (oedema/erythema, redness and/or skin rash) afterwards.

***Ex vivo* skin permeation study**

Ex-vivo skin permeation study was performed using Wistar rat abdominal skin sacrificed upon prolonged anesthesia [33, 35]. Skin hairs were carefully removed using surgical blade while full skin was removed to expose the dermis which was properly rinsed with normal saline to remove residual fat. The skin (thickness 1.5 - 2.5 mm) was fixed on a Franz diffusion cell (PermeGear Inc., Hellertown, PA, USA) with permeation area of 3.14 cm^2 and the receptor compartment was filled with 15 ml ethanol:water mixture (1:1) stirred continuously at 500 rpm at 32 ± 0.5°C. Weighed amount of nanogel (2 g equivalent to 25 mg of ART) was carefully applied to the skin in the donor compartment, evenly spread using flat surface of a spatula to maintain intimacy with the skin. At pre-determined time intervals (10, 20, 40, 60, 80, 100, 120 and 140 h) up to 7 days, 0.5 ml of sample was withdrawn from receptor compartment then replaced with equal volume of fresh diffusion medium, to maintain sink conditions. All samples were filtered through a membrane filter (0.45 μm), diluted appropriately, and analyzed by spectrophotometry (Jasco V-630 UV/VIS Double Beam, Japan), modified as stated above [16]. Briefly, the 0.5 ml withdrawn sample was added to 0.5 ml of concentrated HCl in a test tube, securely stoppered and stood in a water bath at 80 °C for 30 min and afterwards cooled, diluted with distilled water (12.5 ml) and filtered. Absorbance of this solution was taken at 345 nm against a blank solution of HCl (conc, 0.5 ml) made up to 12.5 ml with distilled water. The cumulative

amount of ART permeated per unit area of rat skin was calculated and plotted against time, after reference to a Beer's plot for pure ART in distilled water. The test was repeated using ART-loaded NLC (1.5 g equivalent to 33 mg of ART) as positive control in triplicate. Due to the observed slow release of ART from formulations (NLC and nanogels), sodium azide (0.02 %) was incorporated into the quantities used for skin permeation study, as a preservative in order to extend the release study for one week [36]. As a result, the study was repeated using each nanogel dose of 2 g and sampling was done 24 hourly for 7 days.

***In vivo* transdermal anti-plasmodial (schizonticidal) activity of nanogels**

The *in vivo* anti-plasmodial activity was considered using a 4-day suppressive test procedure (Peters 4-day suppressive test) [18, 37]. Briefly, fifty albino male Wistar mice were divided into 10 groups (1-10) of 5 animals each, weighed and clearly marked to avoid mix-up. Some 24 h prior to experiment, mice dorsal skin was shaved with an electric clipper. Through cardiac puncture, the blood of the donor mice was collected and diluted with physiological saline (normal saline) to give a concentration of 10^8 parasitized erythrocytes per ml. A 0.2 ml volume of the donor mouse erythrocyte equivalent to 2×10^7 parasitized erythrocytes was injected intraperitoneally into each of the experimental mice on day 1 (D_1). Group 1 was treated with 5 mg/kg of artemether (p.o. as positive control). Each transdermal nanogel was uniformly applied (2 g each containing 25 mg of ART) once to the shaved dorsal side of the mice to cover an area of 0.4 cm^2, gradually massaged over 30 min until complete absorption and covered with an adhesive tape to avoid leaking by others. This applied to mice Groups (2-4) corresponding to ART nanogel formulations coded as C971P-ANG, PAPP-ANG and P407-ANG respectively while Group 5 mice were treated with ART-NLC (1.5 g dispersed in 1 ml of 1:1 water-ethanol mixture, equivalent to 33 mg of ART) and applied to the shaved skin area as described shortly. Rat Groups 6-8 were treated with drug-free nanogels from each batch of C971, PAPP and P407 whereas Group 9 was infected but not treated (negative control). Treatments with the formulations were done once in a week after 24 h post-infection whereas Group 10 mice received pure chloroquine phosphate (5 mg/kg, p.o) daily. Afterwards, the animals were subjected to red blood cell count (RBC) and parasitemia count (as *ab initio* determined for the donor mouse). The RBC count was determined using hemocytometer method. Briefly, a mixture of 0.1 mL of animal's blood was mixed with 0.9 mL of Hayems solution and placed in a charged counting chamber whereby the cells were counted as n and multiplication of n by 10,000 was expressed in cells/mm^3 [11]. The parasitemia count was determined by tail-bleeding the mice and preparing

blood smears on microscope slides, subsequently, fastened with methanol and marked with Giemsa. The parasitemia number was determined by viewing under the microscope and taking the count thrice and the average calculated. The antimalarial activity was evaluated using equation below:

$$\text{Plasmodial growth inhibition (\%)} = \frac{MPNC - MPTS}{MPNC} \times 100 \quad \text{..... Eq. (8)}$$

where, MPNC = mean parasitemia of negative control and MPTS = mean parasitemia of test sample

Statistical analysis

All the data generated were expressed as mean ± standard deviation. For group comparisons, one-way ANOVA with duplication was applied. Statistical significance was determined using student t-test, with $p<0.05$ considered to be statistically significant.

Results and discussion

Characterization of NLC particles

It was essential to characterize the NLC particles to ensure reproducibility and compliance to our earlier report. [12]. Our modified method still showed same higher particle size for drug-free NLC (532 nm) than ART-containing NLC (299 nm). Polydispersity index (PI) agreed with this observation as drug-free particles had higher PDI (0.9) compared to ART-loaded particles (0.3). Particle size reduction was observed when freeze-dried NLC particles were reconstituted and stored for 3 months, perhaps indicative of no particle growth, hence suggesting stable particles. This stability was confirmed by the result of zeta potential values which existed well above – 30 mV for both drug-free (-31mV) and ART-loaded (-41 mV) NLC particles. TEM images confirmed near uniform spherical ART-loaded particles better than drug-free particles which appeared somewhat cuboidal (Fig. 1: A and B).

NTA analysis showed absence of microparticles and confirmed that our modified method of preparation gave same value for drug-free NLC (532 nm) at d90 but lower particle size for ART-loaded particles (299 nm) than our earlier report (346 nm) [Fig 1: C and D]. The lower particle size makes our method more attractive for intended transdermal application since particles below 300 nm have been reported to be more ideal for skin uptake [38, 39]. This perhaps could be due to the fact that we used both Transcutol and ethanol as solubilizers. Particle size/Relative

Intensity 3D plot (Fig. 1) confirmed the narrow variation in size of ART-loaded NLC-particles (E) compared to drug-free particles (F).

DSC result is shown in Fig. 2. The 5 % lipid matrix consisting of Gelucire 43/01 (10 %), P85G (15%) and Transcutol (75%) melted at 36.43 °C with enthalpy of 1.940 J/g (A). The same 5 % lipid matrix when containing ART melted at 43.82 °C with enthalpy of 1.087 J/g (B). This indicated that the later was less crystalline than the former judging from enthalpy values. To rule out discrepancy from thermal properties of NLC, D-sorbitol gave a melting point of 102.52 °C with an enthalpy of 1.702 J/g (C), which was also less crystalline than lipid matrix mixture despite having about thrice the melting point of the lipid matrix. ART itself melted at 86.96 °C with an enthalpy of 87.51 J/g (D). This showed that ART is a very crystalline drug whose crystallinity grossly reduced in the 5 % lipid mixture chosen for the study (1.087 J/g), whereby the thermogram shape (B) became somewhat glassy in transition compared to (A). However, NLC formulations (drug-free and ART-loaded) showed two melting peak patterns in their thermograms. The first peak (shoulder) was due to incomplete melting of an amorphous polymorph whereas the second was due to complete melting. For drug-free (blank) NLC, the melting temperatures were 49.29 °C and 82.46 °C with respective enthalpies of 0.1172 J/g and 0.07452 J/g (E). ART-NLC particles melted at 47.88 °C and 96.67 °C with corresponding enthalpies of 0.2138 J/g and 0.02772 J/g respectively (F). Obviously, ART-containing NLC had lower final enthalpy value upon complete melting compared to blank NLC as well as lipid mixture-entrapped ART. This perhaps confirmed that the chosen lipid mixture was suitable to serve as a matrix to solubilize, embed ART and deliver it as NLC regimen. This agrees with the fact that innovative drug delivery system such as NLC is a promising technique to improve solubility, bioavailability and extreme short half-life; hence perhaps could improve dermal penetration and skin retention of ART [12, 33]. NLCs are smart second-generation solid lipid nanoparticles (SLNs) with numerous advantages compared to SLNs and other nanoparticulate colloidal drug delivery systems (liposomes, niosomes, nanoemulsions).

With increased solubility of ART in the lipid matrix and its molecular dispersion in NLC, there is high chances that the encapsulation efficiency would be high. An earlier validated HPLC method was used to study the efficiency of encapsulation of ART in the NLC formulation and the result showed a slightly higher EE of 70 % compared to our earlier report of 61%. Since every processing parameter was nearly the same except for inclusion of ethanol, we could conclusively say that ethanol further enhanced the solubility of ART in the present NLC formulation. We modified this formulation method based on our earlier recommendation following skin permeation

study. Our use of ethanol as co-solubilizer therefore has led to higher drug solubilization and entrapment which invariably would alter drug release profile, improve stability and bioavailability, in addition to localizing delivery through enhanced retention at target site, thereby reducing side effects and dosing frequency, with overall improved patient compliance [12, 40, 41].

Ex vivo tape stripping experiment was done with the ART-NLC formulation. Tape stripping of the skin is a useful tool for removing the *stratum corneum* and obtaining more information about function of this barrier as regards skin penetration. The amount of ART on *stratum corneum* removed by stripped tapes was quantified by UV absorption in 96 well plates (Greiner 96 Flat Bottom Transparent Polystyrol) at wavelength of 282 nm to establish the concentration of ART within the *stratum corneum* after transdermal application (Fig. 3). However, ART was detectable to a large extent in the *SC* through stripping of tapes 1 (~0.5 µg) to 10 (~1.6 µg). Cyanoacrylate biopsy 1 and 2 equally detected much ART (~1.5 µg) as well as skin punch (~1.2 µg) and pipette tips (~0.4 µg). Overall, the highest drug levels were observed mainly in the SC compared to epidermis and dermis according to literature [42]. A repeat analysis with validated HPLC method corroborated the above result. In other words, the formulation likely maintained closer contact with the lipid bilayer of the *stratum corneum* due to its lipid composition and smaller particle size, resulting in penetration of an increased amount of ART into the skin and perhaps controlled release. It is equally expected that skin application of the NLC would produce occlusive effect (improve skin hydration) which could increase penetration of ART across the dermal layers [43-46]. Therapeutic success is dependent on how efficiently ART could reach the target site (which is the blood) to attain effective concentration that could induce the desired schizontocidal activity on blood merozoites. It would therefore be more relevant to determine the concentration of drug at the target site *in vivo* than *ex vivo* since such result is more practicable. Meanwhile, since there was detectable amount of ART penetrating the living epidermis (~1.2 µg) as a positive signal for transdermal systemic delivery into the bloodstream; it could be worth trying to further study the performance of the freeze-dried NLC particles as nanogels on rat skin as well as on malariogenic mice. In the light of the above, NLC particles were entrapped on polymer hydrogels to obtain nanogels which were investigated on rodent models.

Characterization of ART nanogels

pH storage stability

Formulations intended for use on the intact skin (transdermal) require that their pH values comply with the skin pH of 5.5 to avoid any form of skin reaction (irritation, erythema, rash, etc). As a result, the formulation pH was

adjusted after preparation to this optimum value and re-validated each time upon use as well as upon storage up till 6 months (Fig. 4). Briefly, preparations obtained from C971P were highly acidic (1.2) before they were buffered with triethanolamine (in drops) unlike those of P407 that were entirely alkaline (8.0) and the weakly acidic PAPP formulations (6.2). However, there were mild insignificant fluctuations in pH ($p<0.05$) upon storage (especially from 1-week post formulation to 6 months) but more generally, all the formulations were stable for the study period.

Spreadability measurement

Generally, all formulations had excellent spreadability (Table 2). The essence of this measurement was to ensure uniform dose and spread of the formulation upon application on the skin. In order words, the user should not experience any kind of grittiness upon rubbing an applied dose of the formulation on the intact skin. This also shows that the tested polymers (C971P NF, PAPP and P407) all had good gelling properties, especially because they are all water-soluble polymers; hence the ease of formulation. Additionally, they are useful excipients in the industries (cosmetic, food and pharmaceutical); hence they are generally regarded as safe (GRAS) without any reactive or toxic effects [33, 47]. ART-nanogel spreadability decreased in the order of P407> C971P>PAPP corresponding to 540.0 ± 0.23, 455.0 ± 0.08 and 435.0 ± 0.19 % respectively, whereas placebo nanogels (without ART) had higher spreadability values in the order of P407>C971P>PAPP corresponding to 670.0 ± 0.12, 650.0 ± 0.04 and 610.0 ± 0.12 %compared to the plain hydrogels (no NLC) which had the highest spreadability in the order of P407>C971P>PAPP accruing to 705.0 ± 0.06, 700.0 ± 0.07 and 689.0 ± 0.14 % respectively. However, the PAPP formulation consistently showed the least spreadability in each test group, though compared favourably with the standard polymers. C971P NF polymer is a lightly cross-linked polymer with long rheology, which results in flow like honey (high spreadability) in a semi-solid formulation as tested [48]. No doubt the formulations were easily spreadable upon minimal shear/force (rubbing). This at least proves that the formulations are suitable for transdermal use.

***In vitro* occlusivity**

An occlusive formulation is expected to improve skin hydration and prevent transepidermal water loss by thin film formation upon skin application. In other words, this makes for better permeation of drug through opening of corneocyte's tight-junctions [49]. Table 2 shows that ART-nanogels had more occlusion than the placebo and/or plain hydrogel formulations. ART nanogel occlusivity (F) followed the order of P407>PAPP>C971P corresponding to 69, 66 and 60 at 48 h. Change in F at 24 h (55) to 48 h (60) was more pronounced in C791P-ANG than other

formulations. Generally, ART-nanogels have shown that they could expectedly reduce transepidermal water loss upon application on the skin thereby increasing skin hydration and subsequent deposition and penetration of ART.

Rheological determination

Fig 5 shows that the formulations had satisfactory viscosities. There were concentration-independent decreases in viscosity in ART-nanogels formulated from P407 and PAPP unlike in C971P. This perhaps showed that the ART nanogels from both P407 and PAPP had sufficient viscosity even at lower amounts. However, placebo nanogels and plain hydrogels of 407 and PAPP showed concentration-dependent increases in viscosity, still opposite to that observed for C971P. Invariably, the viscoelastic property of semi-solid formulations is somewhat related to spreadability and could reveal how spreadable and/or pourable the formulations could be. This perhaps suggests that a highly viscous preparation would also not easily spread and vice versa. In the light of this, the ART-nanogels would require minimum force/pressure/shear or rubbing to spread upon application on the skin and this supports our observation with the spreadability result.

Drug content analysis

Nanogel formulations demonstrated high ART content in all three polymers (C971P NF, PAPP and P407) as shown in Table 2. Drug content was in the order of P407>PAPP>C971P corresponding to 97, 91 and 88 % ART which showed insignificant change ($p<0.05$) of encapsulated amount even over 6 months storage period [50]. This however agreed with our earlier reports on different delivery systems using these polymers (example spray-dried solid dispersions of aceclofenac using PAPP [28] and gentamicin microgels using P407 and C971P NF [33]). In order words, it corroborates the efficiency of encapsulation of ART in the nanostructured lipid carrier as improving ART oil solubility and delivery properties.

***In vitro* drug release and release mechanism**

Fig. 6 shows the result of *in vitro* ART release from formulations. All formulations showed extended ART release over 3 days without exhausting all embedded drug. However, the membrane-free model of drug release allowed direct contact with the formulations as a way of simulating use condition in real time and place. ART-NLC released up to 50 % ART in 50 h whereas nanogel formulations followed the order of P407>PAPP>C971P corresponding to 41, 40 and 35 % cumulative release of ART over 3 days, with no burst release. This shows that the optimized NLC formulation indeed had good lipid properties, surface modification, drug solubility as well as partition coefficient. All formulations showed slow release pattern which could attest to the high solubilization and hydration rate of the

polymers in release media. This has at least demonstrated that the polymers could serve as competent reservoirs to deliver ART over an extended time period. All ART-nanogels showed similar pattern of release. Table 3 shows the release kinetic models of all formulations. The correlation coefficients (r^2) persistently followed the order of Higuchi>First>Zero>Korsmeyer-Peppas. Therefore, Higuchi square root model of release predominated in all formulations. The release exponent 'n' values were in the range of 0.672 – 0.75. This shows that the mechanism of ART release was non-Fickian diffusion (anomalous) and depended on diffusion rate and/or matrix erosion.

Skin tolerance test

Skin tolerance test was necessary to evaluate the biocompatibility of the transdermal formulations [51]. There was generally no sign of skin reaction (redness/erythema, wrinkling, papules and/or dermatitis) after application (5 days) of all formulations (NLC, plain hydrogel, placebo and ART nanogels), compared to the skin disruptions (erythema and inflammation) observed on rats which received the irritant (formaldehyde solution). This indicated that the formulations were safe for skin use and this good skin tolerability could perhaps be attributed to the GRAS status of all components of the formulation.

***Ex vivo* permeation**

Figs. 7 and 8 showed the cumulative amount of ART permeated and percentage cumulative amount permeated in 7 days from all four-drug loaded formulations respectively. ART-loaded nanogels were tested at 2 g formulation containing 25 mg of ART compared to the ART-NLC which served as positive control and tested at 1.5 g dose containing 33 mg of ART. This dose inequality was based on our earlier tested dose of 30 mg of ART-loaded NLC which credibly released about 3-6 µg of ART over 3 days, achieving about 18 % cumulative drug release [12]. Since there is no standard commercial sample of ART for skin use, we therefore leveraged on this known dose to test our new modified formulations (NLC and nanogels) at 33 and 25 mg doses respectively. We understand there could be species differences (such as skin type, age and hydration parameters) since our earlier permeation tested real human skin whereas our current test used Wistar rat abdominal skin and ethanol as penetration enhancer. Likewise, the precision of our earlier report was based on HPLC analysis whereas herein, we used a derivatized UV/VIS analysis method. Taking everything together, ART still showed prolonged permeation over a 7-day period in the order of ART-NLC>P407-ANG>C971P-ANG>PAPP-ANG cumulatively achieving 15, 12, 10.5 and 7 µg of ART in 7 days. However, ART release was fastest from the PAPP polymer which in 5 days showed highest release of 11 µg ART and later tapered off to 7 µg. Interestingly, this corresponded to 60, 48, 42 and 28 % cumulative ART release at 140

h of the 7th day; with PAPP-ANG exhausting its payload in 5 days with about 44 % ART cumulative release. The enhanced performance of our present investigation may perhaps have come from the use of ethanol:water mixture (1:1) as a penetration enhancer in formulation of the NLC, which even in the nanogel formulation was maintained. This could have additionally boosted the solubilization of ART in the nanogel formulation and could also explain why the present investigation achieved smaller nanoparticles (299 nm) compared to our earlier report of 346 nm [2]. Efficient skin permeation had been described for particles around 300 nm [51]. ART nanogels were henceforth developed with capacity to permeate the intact skin (transdermal) as a positive proof for alternate malaria regimen with improved patient use-convenience (friendliness) other than tablet and/or injection.

Generally, the carefully selected excipients used in the current study somewhat exhibited synergism in the permeation process through the intercellular (paracellular) pathway. Firstly, ethanol as a permeation enhancer has been reported to work by the following mechanisms; (1) increase of diffusivity of the drug in the skin, (2) fluidization of SC, which causes a decrease in barrier function, (3) increasing the thermodynamic activity of the drug in the carrier, and (4) affecting the partition coefficient of the drug [52]. The mechanism of ethanol as a skin permeation enhancer has also been described to be a so-called 'pull' or 'drag' effect, which means that the permeation of the enhancer (ethanol) subsequently facilitates that of the solute, ART (in the sense of a simple co-permeation) [53, 54]. On the other hand, Transcutol HP® (Diethylene Glycol monoethyl Ether, DEGEE) has been reported as a permeation enhancer known to increase the thermodynamic driving force, facilitate partitioning of the drug to maintain hydrated dynamics in the SC and intercellular lipid fluidization [55]. Additionally, other additives in the formulation such as Tween 80 and propylene glycol have equally been reported as penetration enhancers by increasing drug permeation from improved partition properties and reduced drug-tissue binding by the solvation of α-keratin causing disruption within the corneocyte. This affects lipids in the SC by interacting with the aqueous domains of lipid bilayers, changing the solubility of skin and increasing the drug partitioning into it [56]. Summarily, the predominate mechanism of penetration enhancement in this study was by intercellular mechanism through the lipid matrix component of the skin.

In vivo transdermal antiplasmodial study

Percentage reduction in parasitaemia is displayed in Fig. 9. Generally, there was plasmodial growth inhibition across all drug-containing formulations. The parasitized mice responded to chloroquine phosphate and pure ART after oral

administrations and showed up to 75 and ~ 82 % inhibition of paratasitaemia respectively. Skin application of ART-NLC dispersion (1:1 mixture of ethanol:water) compared well with these positive controls ($P<0.01$) by achieving 80 % plasmodial inhibition. ART-nanogels equally demonstrated good plasmodial inhibitions in the order of P407-ANG>PAPP-ANG>C971P-ANG corresponding to 54.36, 54.32 and 47.64 % respectively ($P<0.01$) compared to their respective placebo nanogels which showed 15.26, 14.26 and 16.18 %. The infected but not treated group which received normal saline had no plasmodial reduction at all. This shows that the formulations were able to reduce parasitaemia upon single application cumulatively across some 7 days, perhaps due to the fine particle subdivision (299 nm) that improved ART solubility in the lipid matrix as well as inclusion of ethanol as a penetration enhancer which could have made for better permeation of ART through opening of the corneocyte's tight-junctions [36, 52-54].

This molecular dispersion of ART in the glassy NLC matrix that encapsulated up to 70 % of drug in its very stable (-41 mV) and uniform manner (0.3 PDI) could have boosted this observation. Meanwhile, this work has at least proved the feasibility of transdermal delivery of ART using NLC and NLC-derivatized nanogels as low-dose transdermal regimens. However, since a single skin patch application (25 mg ART) achieved about 50% plasmodium growth inhibition in a prolonged period of seven days as further confirmed by the microscopy, we assure that increasing the patch application to two skin patches (50 mg ART) concurrently would provide near 100% plasmodial growth inhibition in seven days. This double patch dose of 50 mg ART is still lower (near half-dose) than the conventional regimens available in the drug market. Additionally, the present investigation has also shown that the use of the local water-soluble polymer from *Prosopis africana* peel powder (PAPP) compared well with pharmaceutical standards (Poloxamer 407 and Carbopol 971P NF) in delivery of the poorly water-soluble drug such as artemether. As an outlook, further studies could be recommended to quantify ART in different layers of the skin.

Conclusion

This study authenticates NLC as a delivery system for ART both orally and transdermally. Optimized ART concentration (250 mg) was molecularly dispersed in glassy NLC matrix that encapsulated up to 70 % of drug in its very stable (-41 mV) fine spherical particle subdivisions (299 nm) in a uniform manner (0.3 PDI). *Ex vivo* tape stripping of pig ear skin showed reasonable drug concentration in the living epidermis and/or dermis even though higher in the *stratum corneum*. ART-nanogels had good pH storage stability, viscosity, spreadability, drug content, *in vitro* drug release, skin tolerance and occlusivity leaving a thin-film after application on the skin due to good

hydration and ability to prevent skin transepidermal water loss. *Ex vivo* skin permeation showed that reasonable amounts of ART permeated through the rat abdominal skin in the order of ART-NLC>P407-ANG>C971P-ANG>PAPP-ANG achieving cumulative permeations of 15, 12, 10.5 and 7 µg in 7 days, corresponding to cumulative percentage permeations of 60, 48, 42 and 28 % respectively ($P<0.01$). The *in vivo* transdermal anti-plasmodial study of single skin patch application (25 mg ART) equally maintained the order with 80, 54, 54 and 48 % respective inhibition of plasmodial growth in 7 days ($P<0.01$). This study has demonstrated some proof of concept that ART definitely permeated through the intact skin (*ex vivo* and *in vivo*) into the living epidermis (blood) and/or dermis by intercellular pathway and could be a potential alternative regimen with better use convenience than frequent injection and/or tablet administration. This could therefore correct the negative attitude associated with the many side-effects of the conventional ART-containing regimens in ACT which is responsible for the growing resistance to artemisinin currently. In extrapolation therefore, multiple concurrent application of the formulated nanogels (i. e. two-patches/week, 50 mg ART) would inhibit plasmodial growth by near 100% and hence, cure malaria completely. In this way, the ordinarily fast-acting schizonticide ART (100 mg or more, with short half-life, 1.5-3/5 h) has been transformed into a lower-dose (50 mg ART, upon multiple patch application) prolonged-release-friendly regimen which would take care of recrudescence and development of resistance usually observed with the conventional single forms of ART and/or artemisinin, which the use of ACT as recommended by the WHO was meant to take care off. However, further permeation studies could be required to precisely quantify the specific amounts of ART in the different layers of the skin.

Conflict of interest

All authors (Petra O. Nnamani, Agatha A. Ugwu, Ogechukwu H. Nnadi, Franklin C. Kenechukwu, Kenneth C. Ofokansi, Anthony A. Attama, Claus-Michael Lehr) declare that they have no conflict of interest in the work done.

Acknowledgement

Prof. P. O. Nnamani is grateful to the Tertiary Education Trust Fund (TETFund) (Grant no. TETFUND/DESS/UNI/NSUKKA/RP/VOL.V) by Government of Nigeria for funding the research through Institution-Based Research.

ORCID

Petra O. Nnamani ID: http://orcid.org/0000-0001-9677-1288

ETHICAL STATEMENT:

o Ethics approval and consent to participate: 'All institutional and national guidelines for the care and use of laboratory animals were followed.' Approval was obtained from Animal Care and Use Committee of the Faculty of Pharmaceutical Sciences (approval no. FPSRE/UNN/18/00036), in compliance with the EU Directive 2010/63/EU for animal experiments.

o Consent for publication: All Authors agree that the contents of the manuscript are confidential and will not be copyrighted, submitted, or published elsewhere (including the internet), in any language, while acceptance by the Journal is under consideration. All authors made substantial contributions to the conception or design of the work; or the acquisition, analysis, and/or interpretation of data; drafted the work or revised it critically for important intellectual content as well as approved the version to be published.

o Availability of data and materials: All data and materials as well as software application support our published claims and comply with field standards. Our paper was earlier presented as an oral paper (NAPA2020-104) during the recent concluded 18th National scientific conference of the Nigeria Association of Pharmacists in academia (NAPA) held at the University of Nigeria Nsukka from 24th -26th August, 2020 but not under submission for publication anywhere except in DDTR.

o Competing interests: Not applicable

o Funding: Tertiary Education Trust Fund (TETFund) (Grant no. TETFUND/DESS/UNI/NSUKKA/RP/VOL.V) by Government of Nigeria for funding the research through Institution-Based Research.

o Authors' contributions: All authors contributed to the study conception and design. Material preparation, data collection and analysis were performed by [Ugwu AA], [Nnadi OH], [Kenechukwu FC] and [Ofokansi KC]. The first draft of the manuscript was written by [Nnamani PO] and all authors commented on previous versions of the manuscript. All authors read and approved the final manuscript [Attama AA] [Claus-Michael Lehr]

o Acknowledgements: Prof PO Nnamani acknowledges support by the Tertiary Education Trust Fund (TETFund) (Grant no. TETFUND/DESS/UNI/NSUKKA/RP/VOL.V) by Government of Nigeria for funding the research through Institution-Based Research.

o Authors' information (optional): Prof. Dr. Petra Obioma Nnamani is Senior Lecturer at Department of Pharmaceutics, University of Nigeria Nsukka (UNN). Dr. Nnamani studied pharmacy in UNN (B. Pharm; 2001) and M. Pharm (2004). During her Ph.D (2006-2010), Petra joined the nanotechnology group at ICS-UNIDO Trieste, Italy (2009) for Early Research Training in Nanotechnology. She obtained her Ph.D (2010) in Drug Delivery and has had postdoctoral trainings in Shivaji University Kolhapur, India (2012) and Helmholtz-Institute for Pharmaceutical Research Saarland (HIPS), Saarland University, Germany (2013) and currently a Georg Forster awardee of the Alexander von Humboldt Stiftung, AvH (2019-2020). Her research focuses on exploring the biological barriers of gastrointestinal tract and the skin, using nanotechnology-based drug carriers capable of crossing epithelial barriers and sustaining drug release in different disease conditions. Prof. Nnamani is recipient of several awards: Georg Forster Award of AvH, 1 of 10 women innovators in African continent by World Intellectual Property Organization/Innovation Prize for Africa, Botswana 2016; Grand Challenges Canada Star in Global Health (2013-2015), Leader is STEM 2017 (TechWomen). She has 75 published papers; 41 conference contributions; mother of 5 children and journal reviewer.

References

1. WHO Global malaria programme. Geneva, World Malaria Report, 2019. (ISBN 978-92-4-156572-1) Switzerland. (https://www.who.int/malaria).

2. Wong YK, Xu C, Kalesh KA, He Y, Lin Q, Wong WSF, Shen H-M, Wang J. Artemisinin as an anticancer drug: Recent advances in target profiling and mechanisms of action. Med Res Rev. 2017;37:1492–1517. doi: 10.1002/med.21446

3. Li Y. Qinghaosu (artemisinin): chemistry and pharmacology. Acta Pharmacol Sin. 2012;33:1141–1146. doi: 10.1038/aps.2012.104

4. Looa CSN, Lama NSK, Yua D, Sub X-z, Lud F. Artemisinin and its derivatives in treating protozoan infections beyond malaria. Pharmacol Res. 2017;117:192–217. doi:10.1016/j.phrs.2016.11.012.

5. Appalasamy S, Lo KY, Ch'ng SJ, Nornadia K, Othman AS, Chan L-K. Antimicrobial activity of artemisinin and precursor derived from *in vitro* plantlets of Artemisia annua L. BioMed research international. 2014 doi: 10.1155/2014/215872.

6. Roy S, He R, Kapoor A, Forman M, Mazzone JR, Posner GH, Arav-Boger R. Inhibition of human cytomegalovirus replication by artemisinins: effects mediated through cell cycle modulation. Antimicrobial agents and chemotherapy. 2015;59(7):3870–3879. DOI: 10.1128/AAC.00262-15

7. Blazquez AG., Fernandez-Dolon M, Sanchez-Vicente L, Maestre AD, Gomez-San Miguel AB., Alvarez M, Serrano MA., Herwig J, Efferth T, Marin JJG, Romero MR. Novel artemisinin derivatives with potential usefulness against liver/colon cancer and viral hepatitis. Bioorganic & Medicinal Chemistry. 2013;21:4432–4441.

8. Pfeifhofer-Obermair C, Tymoszuk P, Petzer V, Weiss G, Nairz M. Iron in the tumor microenvironment—connecting the dots. Front Oncol. 2018;8:549. doi: 10.3389/fonc.2018.00549.

9. Zhang Y, Xu G, Zhang S, Wang D, Prabha PS, Zuo Z. Antitumor research on artemisinin and its bioactive derivatives. Nat Products Bioprospect. 2018;8:303–319. doi: 10.1007/s13659-018-0162-1.

10. Wang J, Zhang CJ, Chia WN, Loh CC, Li Z, Lee YM, He Y, Yuan L-X, Lim TK, Liu M, Liew CX, Lee YQ, Zhang J, Lu N, Lim CT, Hua Z-C, Liu B, Shen H-M, Tan KSW, Lin Q. Haemactivated promiscuous targeting of artemisinin in Plasmodium falciparum. Nat Commun. 2015;6:10111. doi: 10.1038/ncomms10111.

11. Deng T, Wang X, Wu S, Hu S, Liu W, Chen T, Yu Z, Xu Q, Liu F. A new FRET probe for ratiometric fluorescence detecting mitochondria-localized drug activation and imaging endogenous hydroxyl radicals in zebrafish. Chem Commun. 2020;56:4432–4435. doi: 10.1039/D0CC00382D.

12. Nnamani PO, Hansen S, Windbergs M, Lehr CM. Development of artemether-loaded nanostructured lipid carrier (NLC) formulation for topical application. Int J Pharm. 2014;477:208–217. doi: 10.1016/j.ijpharm.2014.10.004.

13. Aderibigbe AB. Design of drug delivery systems containing artemisinin and its derivatives. Molecules 2017;22:323. doi: 10.3390/molecules22020323

14. Nnamani PO, Scoles G, Kröl S. Preliminary characterization of N-trimethylchitosan as a Nanocarrier for Malaria Vaccine. J Vector Borne Disease. 2011;48(4):224-230. PMID: 22297285; DOI: 10.1186/1758-2946-4-s1-p47

15. Attama AA, Kenechukwu FC, Onuigbo EB, Nnamani PO, Obitte NC, Finke JH, Pretor S, Müller-Goymann CC. Solid lipid nanoparticles encapsulating a fluorescent marker (coumarin 6) and antimalarials – artemether and lumefantrine: evaluation of cellular uptake and antimalarial activity. European Journal of Nanomedicine. 2016;8(3)129–138, ISSN (Online) 1662-596X, ISSN (Print) 1662-5986, DOI: 10.1515/ejnm-2016-0009.

16. Nnamani PO, Ugwu AA, Ibezim EC, Kenechukwu FC, Akpa PA, Ogbonna JDN, Obitte NC, Lehr CM, Attama AA. Sustained-release Liquisolid Compact Tablets Containing Lumefantrine-Artemether as Alternate-Day-Regimen for Malaria Treatment to Improve Patient Compliance. International Journal of Nanomedicine. 2016;11:6365-6378. doi: 10.2147/IJN.S92755.

17. Nnamani PO, Nnadi OH, Ibezim EC, Ayogu E, Reginald-Opara JN, Onoja US, Odo AN, Ugwu AA, Ogbonna CC, Attama AA. *In vivo* antiplasmodial potential of Carrageenan and *Prosopis africana* buccal films of artemether on malariogenic mice. Journal of Drug Delivery & Therapeutics. 2020;10(1-s):114-125. DOI https://doi.org/10.22270/jddt.v10i1-s.3790

18. Nnamani PO, Echezona AC, Metu OC, Onoja US, Ogbonna JDN, Akpa PA, Onunkwo GC, Nzekwe IT, Attama AA. Formulation and characterization of artemether-loaded sodium alginate microcapsules. Tropical Journal of Pharmaceutical Research 2020;19 (7):1341-1349 ISSN: 1596-5996 (print); 1596-9827 (electronic) http://dx.doi.org/10.4314/tjpr.v19i7.1

19. Nnamani PO, Hansen S, Lehr CM. Preparation and characterization of artemether-loaded PLGA nanoparticles. Afr J Pharm Res Dev. 2018;10:1-10.

20. Jabbarzadegan M, Rajayi H, Jahromi MAM, Yeganeh H, Yousefi M, Hassan ZM, Majidi J. Application of arteether-loaded polyurethane nanomicelles to induce immune response in breast cancer model. Artif Cells Nanomed Biotechnol. 2017;45:808–816. doi: 10.1080/21691401.2016.1178131

21. Agubata CO, Nzekwe IT, Attama AA, Mueller-Goymann CC, Onunkwo GC. Formulation, characterization and anti-malarial activity of homolipid-based artemether microparticles. Int J Pharm. 2014;14483:1–21. http://dx.doi.org/10.1016/j.ijpharm.2014.11.044

22. Tran HT, Nguyen TD, Nguyen HV, Nguyen HT, Kim JO, Yong CS, Nguyen CN. Targeted and controlled drug delivery system loading artersunate for effective chemotherapy on CD44 overexpressing cancer cells. Arch Pharm Res. 2016;39:687–694. doi: 10.1007/s12272-016-0738-4.

23. Akbarian A, Ebtekar M, Pakravan N, Hassan ZM. Folate receptor alpha targeted delivery of artemether to breast cancer cells with folatedecorated human serum albumin nanoparticles. Int J Biol Macromol. 2020;152:90–101. doi: 10.1016/j.ijbiomac.2020.02.106.

24. Charlie-Silva I, Fraceto LF, de Melo NFS. Progress in nano-drug delivery of artemisinin and its derivatives: towards to use in immunomodulatory approaches. Artif Cells Nanomed Biotechnol. 2018;46:S611–S620. doi: 10.1080/21691401.2018.1505739.

25. Kalepu S, Nekkanti V. Insoluble drug delivery strategies: review of recent advances and business prospects. Acta Pharmaceutica Sinica B. 2015;5:442–453. doi: 10.1016/j.apsb.2015.07.003

26. Patra JK, Das G, Fraceto LF, Campos EVR, Rodriguez-Torres MDP, Acosta-Torres LS, Diaz-Torres LA, Grillo R, Swamy, MK, Sharma S, Habtemariam D, Shin H-S. Nano based drug delivery systems: recent developments and future prospects. J Nanobiotechnology 2018;16:71. doi: 10.1186/s12951-018-0392-8.

27. Wilkhu JS, McNeil SE, Anderson DE, Kirchmeier M, Perrie Y. Development of a solid dosage platform for the oral delivery of bilayer vesicles. European Journal of Pharmaceutical Sciences. 2017;108:71–77.

28. Nnamani PO, Lokhande CD, Shinde AJ, Jadhav NR, Sanandam MR. *SOLID ORAL PHARMACEUTICAL COMPOSITION.* Nigerian patent 2014;565:NG/PT/NC/2014/565.

29. Filipe V, Hawe A, Jiskoot W. Critical evaluation of nanoparticle tracking analysis (NTA) by NanoSight for the measurement of nanoparticles and protein aggregates, Pharm Res.2010;27:796–810.

30. Hansen S, Henning A, Naegel A, Heisig M, Wittum G, Neumann D, Kostka KH, Zbytovska J, Lehr CM, Schaefer UF. In-silico model of skin penetration based on experimentally determined input parameters. Part I: Experimental determination of partition and diffusion coefficients. Eur J Pharm Biopharm. 2008;68:352–367.

31. Lademann J, Jacobi U, Surber C, Weigmann HJ, Fluhr JW. The tape stripping procedure – evaluation of some critical parameters, Eur J Pharm Biopharm. 2009;72:317–323.

32. Borgia SL, Regehly M, Sivaramakrishnan R, Mehnert W, Korting HC, Danker K, Roder B, Kramer KD, Schäfer-Korting M. Lipid nanoparticles for skin penetration enhancement-correlation to drug localization within the particle matrix as determined by fluorescence and parelectric spectroscopy, J Control Rel. 2005;110:151–163.

33. Nnamani PO, Kenechukwu FC, Dibua EU, Ogbonna CC, Monemeh UL, Attama AA. Transdermal microgels of gentamicin. Eur J Pharm Biopharm. 2013;84:345-354. doi: 10.1016/j.ejpb.2012.11.015.

34. Shen CY, Xu PH, Shen BD, Min HY, Li XR, Han J, Yuan HL. Nanogel for dermal application of the triterpenoids isolated from *Ganoderma lucidum* (GLT) for frostbite treatment. Drug Deliv. 2016;23:610-618. https://doi.org/10.3109/10717544.2014.929756

35. Sharma G, Dhankar G, Thakur K, Raza K, Katare OP. Benzyl benzoate-loaded microemulsion for topical applications: Enhanced dermatokinetic profile and better delivery promises. AAPS Pharm Sci Tech. 2016;7:1222-1231. https://doi.org/10.1208/s12249-015-0464-0

36. Ruela ALM, Perissinato AG, de Sousa Lino ME, Mudrik PS, Pereira GR. Evaluation of skin absorption of drugs from topical and transdermal formulations. Brazilian Journal of Pharmaceutical Sciences 2016;52(3) http://dx.doi.org/10.1590/S1984-82502016000300018.

37. Robinson BL, Tovey G, Rossier JC, Jefford CW. The chemotherapy of rodent malaria. The activities of some synthetic 1 , 2 , 4-trioxanes against chloroquine-sensitive and chloroquine-resistant parasites . Part 3 : Observations on ‘ Fenozan-50F ’, a The ch. Annals Trop Med Parasit. 1993;87:111-123.

38. Allen Jr. LV. Transdermals: the skin as part of a drug delivery system, Int J Pharm Compound. 2011;15(4):308–315.

39. Hansen S, Henning A, Naegel A, Heisig M, Wittum G, Neumann D, Kostka KH, Zbytovska J, Lehr CM, Schaefer UF. In-silico model of skin penetration based on experimentally determined input parameters. Part I: Experimental determination of partition and diffusion coefficients, Eur J Pharm Biopharm. 2008;68:352–367.

40. Souto EB, Wissing SA, Barbosa CM, Muller RH. Development of a controlled release formulation based on SLN and NLC for topical clotrimazole delivery. Int J Pharm. 2004;271:71–77 https://doi.org/10.1016/j.ijpharm.2004.02.032

41. Radtke M, Souto EB, Muller RH. Nanostructured lipid carriers: a novel generation of solid lipid drug carriers. Pharm Technol Eur. 2005;17:45–50

42. Pople PV, Singh KK. Development and evaluation of colloidal modified nanolipid carrier: Application to topical delivery of tacrolimus, Part II – *In vivo* assessment, drug targeting, efficacy, and safety in treatment for atopic dermatitis. Eur J Pharm Biopharm. 2013;84:72–83.

43. Rajinikanth PS, Chellian J. Development and evaluation of nanostructured lipid carrier-based hydrogel for topical delivery of 5-fluorouracil. Int J Nanomed. 2016;11:5067-5077. https://doi.org/10.2147/IJN.S117511

44. Tiwari S, Mistry P, Patel V. SLNs based on co-processed lipids for topical delivery of terbinafine hydrochloride. J Pharm Drug Dev. 2014;1:404. https://doi.org/10.15744/2348-9782.1.604

45. Yang X, Zhao L, Almasy L, Garamus VM, Zou A, Willumeit R, Fan S. Preparation and characterization of 4-dedimethylamino sancycline (CMT-3) loaded nanostructured lipid carrier (CMT-3/NLC) formulations, Int J Pharm. 2013;450:225–234. https://doi.org/10.1016/j.ijpharm.2013.04.021

46. Vaghasiya H, Kumar A, Sawant K. Development of solid lipid nanoparticles based controlled release system for topical delivery of terbinafine hydrochloride. Eur J Pharm Sci. 2013;49:311–322. https://doi.org/10.1016/j.ejps.2013.03.013.

47. Nnamani PO, Shinde AJ, Jadhav NR, Sanandam MR, Lokhande CD. Fundamental properties of *prosopis africana* peel powders (PAPPs) as drug delivery excipient. Afr J Pharm Res Dev. 2020;12(1):119-133.

48. BF Goodrich Brochure. https://www.lubrizol.com/Health/Pharmaceuticals/Excipients/Carbopol-Polymer-Products/Carbopol-971P-NF-Polymer

49. Shrotriya S, Ranpise N, Satpute P, Vidhate B. Skin targeting of curcumin solid lipid nanoparticles-engrossed topical gel for the treatment of pigmentation and irritant contact dermatitis. Artif. Cells Nanomed Biotechnol. 2017;46:1-12. http://dx.doi.org/10.1080/21691401.2017.1373659

50. Elnaggar YSR, Talaat SM, El-Din MB, Abdallah OY. Novel lecithin-integrated liquid crystalline nanogels for enhanced cutaneous targeting of terconazole: development, *in vitro* and *in vivo* studies. Int J Nanomed. 2016;11:5531-5547. https://doi.org/10.2147/IJN.S117817.

51. Divya G, Panonnummal R, Gupta S, Jayakumar R, Sabitha M. Acitretin and aloe-emodin loaded chitin nanogel for the treatment of psoriasis. Eur J Pharm Biopharm. 2016;107:97-109. http://dx.doi.org/10.1016/j.ejpb.2016.06.019.

52. Uchida, N.; Yanagi, M.; Hamada, H. Physical Enhancement? Nanocarrier? Current Progress in Transdermal Drug Delivery. Nanomaterials 2021, 11, 335. https:// doi.org/10.3390/nano11020335

53. Heard CM, Kung D, Thomas CP: Skin penetration enhancement of mefenamic acid by ethanol and 1,8-cineole can be explained by the 'pull' effect. Int J Pharm 2006, 321:167-170.

54. Heard CM, Screen C: Probing the permeation enhancement of mefenamic acid by ethanol across full-thickness skin, heat separated epidermal membrane and heat-separated dermal membrane. Int J Pharm 2008, 349:323-325.

55. Osborne DW, Musakhanian J. (2018). Skin penetration and permeation properties of transcutol(R)-neat or diluted mixtures. AAPS PharmSciTech 19:3512–33.

56. Vasyuchenko, E.P.; Orekhov, P.S.; Armeev, G.A.; Bozdaganyan, M.E. CPE-DB: An Open Database of Chemical Penetration Enhancers. Pharmaceutics 2021, 13, 66. https://doi.org/ 10.3390/pharmaceutics13010066